THE ASTROPHYSICAL JOURNAL, 323:456–467, 1987 December 15

WHAT HEATS THE HOT PHASE IN ACTIVE NUCLEI?[1]

WILLIAM G. MATHEWS
Lick Observatory and Board of Studies in Astronomy and Astrophysics, University of California, Santa Cruz

AND

GARY J. FERLAND
Astronomy Department, Ohio State University
Received 1987 January 12; accepted 1987 June 17

ABSTRACT

We summarize some constraints on the continuum in active galactic nuclei and discuss implications for the hot intercloud medium. Recent observations of the near ultraviolet, far-infrared, and soft X-ray continuum of these objects, combined with emission-line measurements, suggest that the continuum may actually peak in the 200–1000 Å region. The resulting Compton temperature is $\sim 10^7$ K, far too low for broad-line clouds to be stable against drag forces, or for the hot phase to be optically thin to X-ray radiation.

It is also difficult to reconcile the Compton two-phase model with gas dynamics in the broad-line region. Attempts to form broad-line clouds from condensations in the hot phase may fail since the coolest, densest parts of incipient condensations are subject to disruptive radial forces. In any case, broad-line clouds are expected to become optically thin from Rayleigh-Taylor instabilities as they attempt to move through the hot phase. Typical clouds are essentially frozen into the more massive intercloud medium which must acquire a velocity field consistent with observed line profiles. Compton-heated winds are unable to attain $\sim 10^4$ km s^{-1} unless additional sources of energy density or momentum exist in addition to Compton effects. Compton-heated radial accretion flows are sensitive to initial conditions at large radii; they also lead to emission-line profile cores produced by clouds having inappropriately low densities and have overall profiles that may differ systematically between Seyferts and quasars.

The currently popular picture in which broad-line region clouds are in pressure equilibrium with a hot phase at the Compton temperature must be modified; other heat sources may be at work, or the situation may be controlled by other physics. We discuss possible heating sources for the intercloud medium, as well as some dynamical problems with the current picture.

Subject headings: galaxies: nuclei — radiation mechanisms

I. INTRODUCTION

The emission-line spectra of active galactic nuclei (AGNs) promise to reveal details about the environment within the inner regions and may someday provide useful indicators of such parameters as distance to the host galaxy (Baldwin 1977) or chemical composition of the emitting gas (Shields 1976). Unfortunately it is now clear that even the simplest interpretation of the emission-line spectrum must include a prominent role for inhomogeneities; narrow emission lines appear to radiate near their critical densities (de Robertis and Osterbrock 1986), indicating that gas with a variety of densities must contribute to the net narrow emission-line spectrum. It seems doubtful that the situation in the broad-line region (BLR) is any simpler. This circumstance is unfortunate because a detailed understanding of the spectrum then requires an understanding of the cloud geometry and of the physics governing the formation of clouds at various densities and distances from the central object.

An early clue to the nature of the physics governing cloud formation came from the observation that the so-called "ionization parameter," the ratio of ionizing photons to hydrogen nuclei, seems to be constant from object to object (Davidson 1977; Davidson and Netzer 1979; Baldwin and Netzer 1978). This fact must be a boundary condition for any model which attempts to explain why and how clouds form. The most popular model today is the two-phase equilibrium scenario similar to that proposed by Spitzer (1978) for the local interstellar medium (see McCray 1979; Krolik, McKee, and Tarter 1981; Lepp *et al.* 1985; Kallman and Mushotzky 1985). In this picture the hot phase is at the "Compton temperature" of the radiation field, the temperature where heating due to Compton scattering, and cooling due to the inverse effect, balance.

Compton scattering is not the only possible heat source for the hot phase (see Mathews 1974, 1976; Krolik, McKee, and Tarter 1981). Other processes, such as turbulence, cosmic rays, and radio frequency heating, can also contribute. These must also be considered if it can be shown that the Compton effect is unable to sustain the hot phase at a high-enough temperature for drag forces on BLR clouds to be negligible or for the hot phase to optically thin to observed radiations.

The point of this paper is threefold: the first is to summarize the current thinking regarding the continuum of AGNs. There is now good evidence that the peak of the energy distribution may actually occur in the extreme ultraviolet 200 Å $\leq \lambda \leq$ 1000 Å. Second, we show that the Compton temperature is $T_C \approx 10^7$ K, far too low for BLR clouds to be stable against drag forces, or for the hot phase to be optically thin to observed X-rays. Finally, we discuss some dynamical problems with current models of the intercloud medium.

[1] *Lick Observatory Bulletin*, No. 1077.

II. THE CONTINUUM

In this section we derive a mean continuum by combining direct observations, where they are available, with inferences based on the emission-line spectrum. The following discussion will center on "classical" quasars, which we define to include both radio-loud and radio-quiet objects. There is evidence that the continuous emission from the two classes of objects is not identical (Zamorani *et al.* 1981). However, both radio-loud and radio-quiet objects have broad lines, so radio properties cannot be a deciding issue in BLR cloud formation. We derive a mean spectrum without regard to radio properties.

a) *Infrared, Optical, and Ultraviolet Continuum*

The shape of this continuum has been considered by, among others, Neugebauer *et al.* (1979), Malkan and Sargent (1982), Neugebauer *et al.* (1984), and Oke, Shields, and Korycansky (1984). Two major problems occur over this spectral range. The first is interstellar reddening and has been discussed, for instance, by Malkan (1984). The second is diffuse reemission by the BLR, which can contribute Balmer continuum and Fe II emission (see, for example, Oke *et al.* 1984; Wills, Netzer, and Wills 1985). Neugebauer *et al.* (1979), Oke *et al.* (1984), and Wills *et al.* (1985) conclude that the optical to ultraviolet continuum can be approximated as a powerlaw, that is,

$$f_\nu = a\nu^{-\alpha} ,$$

where $\alpha \approx 0.5$. A power law with this spectral index is drawn in Figure 1, extending between ~ 400 and 1000 Å.

Neugebauer *et al.* (1979) found that continua tended to have a steeper slope in the near-infrared ($1\ \mu m \leq \lambda \leq 3\ \mu m$) that characterizes the optical. In fact, Malkan (1984) found that the near-infrared continuum ($\lambda \approx 3.5\ \mu m$) was well correlated with the 2 keV X-ray continuum (see also Elvis and Lawrence 1984). Malkan noted that the infrared continuum was better correlated with the X-ray luminosity than several other quantities, such as the emission-line spectrum. Finally, Neugebauer *et al.* (1984) find $\alpha \approx 1$ over the interval $10\ \mu m \leq \lambda \leq 100\ \mu m$. Radio-loud objects continue with this spectral index into radio wavelengths (1 cm) while radio-quiet objects must undergo a break somewhere near 1 mm (see Neugebauer *et al.* 1984).

For simplicity we fit the continuum with $\lambda \geq 4400$ Å with a single power law, with a slope of unity, normalized to produce Malkan's observed ratio of 3.5 μm–2 keV luminosities. The fact that we do not incorporate a steeper than unity spectral index in the near-infrared means that we will overestimate the Compton temperature in the following discussion. We assume that the far-infrared continuum ends abruptly at 1 mm.

b) *X-Ray and γ-Ray Continuum*

High-energy continua are parameterized by α_{ox}, the spectral index between 2500 Å and 2 keV (see Zamorani *et al.* 1981), and the local spectral index measured at X-ray energies. Almost all active nuclei are parameterized by essentially the same hard X-ray continuum (see Mushotzky *et al.* 1980; Mushotzky 1982), which can be fitted by a single power law with spectral index 0.7. This, in part, is a selection effect; a diversity of soft X-ray spectra are found (Elvis, Wilkes, and Tananbaum 1985; Elvis and Lawrence 1985), and the value of 0.7 is among the flattest slopes commonly encountered; early samples found X-ray "loud" active nuclei.

We use a typical value of $\alpha_{ox} \approx 1.4$ (Zamorani *et al.* 1981), and the more energetic X-ray slope of the hard X-ray bright objects (0.7). If anything, this continuum is too energetic, so that we will overestimate the Compton temperature in the following section. Finally, there is now evidence that a soft X-ray excess may occur at energies well below 1 keV (see the review by Elvis 1986).

Few active nuclei have been detected as γ-ray sources. If the X-ray continuum is continued to γ-ray energies with an energy slope of 0.7, then the hard X-ray–γ-ray background would be exceeded for currently assumed AGN space densities (see Rothschild *et al.* 1983). It is not now known with certainty just where the high-energy continuum changes slope or starts to roll over. Cen A has been detected at energies up to 0.5 MeV (Gehrels *et al.* 1984), and its spectrum continues as an extrapolation of the lower energy X-ray continuum, a power law with

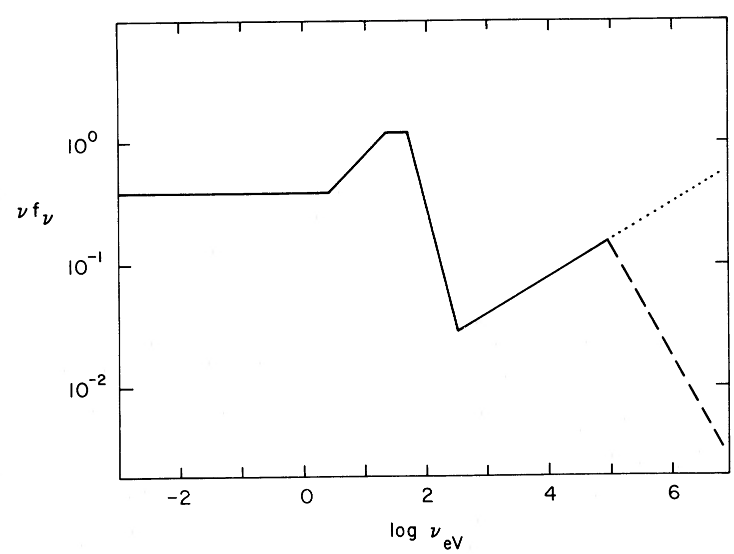

FIG. 1.—Infrared to γ-ray continuum used in the present calculations. Lower axis gives the energy in electron volts, while the upper is the wavelength in Å or μm. Properties of this continuum are also summarized in Table 1.

spectrum index of 0.7. These authors also summarize evidence that the spectrum of Cen A probably undergoes a break between 100 keV and 10 MeV. Baity *et al.* (1984) summarize evidence that the spectral index may increase at 50 keV in NGC 4151 when this Seyfert galaxy is in a high state. *COS B* observations of the quasar 3C 273 (Bignami *et al.* 1981) suggest that the rollover occurs at energies near 1 MeV; however, this object has anomalously strong high-energy emission.

The requirement that active nuclei not exceed the 60–400 keV diffuse background led Rothschild *et al.* (1983) to consider a break in the continuum above 50 keV, to an energy index of 1.67. They found that this form was not inconsistent with their data. We will assume that the break occurs at 100 keV, and that the spectral index above the break is 1.67 (Fig. 1). This assumption is a major source of uncertainty in our determination of T_C; other assumptions concerning the high-energy portion of the continuum will be discussed below.

c) *Extreme Ultraviolet Continuum*

Fabian *et al.* (1986) summarize evidence that the energy distribution of some Seyfert 1 galaxies may peak in the extreme ultraviolet (XUV). Their work was stimulated by the *EXOSAT* observations by Arnaud *et al.* (1985) of a soft X-ray excess in Mrk 841. Fabian *et al.* noted that two stable phases did not occur in this situation and then suggested that this XUV excess may not be seen in the BLR. This might occur, for instance, if the geometry is not spherical, but rather a disk.

It is also possible to infer the properties of the extreme ultraviolet continuum from the BLR emission-line spectrum. In this case the continuum inferred is that which actually strikes BLR clouds and results in ionization of the gas. Two arguments will be used; one based on the equivalent width of He II λ1640 (MacAlpine 1981; MacAlpine *et al.* 1985) and the other based on energy-balance (Netzer 1985). We show that the energy distribution, as seen by the BLR, probably does peak in the XUV.

An estimate of the flux at 4 Ry (228 Å) is made following MacAlpine *et al.* (1985). The mean equivalent width of He II λ1640 in Uomoto's (1984) sample of intermediate redshift quasars is 6.8 Å. If the continuum shortward of 228 Å is approximated as a power law, then it can be easily shown that the number of ionizing photons in the He^+ ionizing continuum is $Q(He^{++}) = f_4/h\alpha$, where f_4 is the flux density, per frequency interval, at 228 Å = 4 Ry, h is Planck's constant, and α is the slope of the power-law continuum between 4 Ry and the X-rays. A steep slope ($\alpha \approx 3$) is needed if the high-energy portion of this continuum is not to exceed the observed X-ray continuum. Assuming case B conditions for the He II lines and letting $\Omega/4\pi$ be the covering factor, we find

$$W_\lambda(\text{He II } \lambda 1640) = \frac{f_\nu(\lambda 228)}{f_\nu(\lambda 1640)} \frac{813}{\alpha} \left(\frac{\Omega}{4\pi}\right)^{-1} = 6.8 \text{ Å} .$$

We assume a covering factor of 10% (Baldwin and Netzer 1978; Smith *et al.* 1981). The resulting continuum is drawn in Figure 1 as a power law extending from 220 Å to join the X-ray continuum at 365 eV. This inferred XUV excess is very similar to that found by Fabian *et al.* (1986) from direct observation of soft X-ray emission from Mrk 841.

Last, we need to consider the continuum between 1 Ry and 4 Ry. This continuum must be fairly flat, both from energy-balance (Netzer 1985) and continuity (Fig. 1) considerations. We extend the ultraviolet ($\lambda > 912$ Å) continuum, with slope 0.5, to $\sim$520 Å. We assume $f_\nu \propto \nu^{-1}$ for the extreme ultraviolet continuum and join this with the He^+ ionizing continuum at 220 Å. The final continuum is shown in Figure 1 and summarized in Table 1. (The energies of the interval boundaries do not exactly agree with the wavelengths given above because of roundoff errors; the continuum used in the calculations below is given exactly by the broken power laws in Table 1.)

III. THE COMPTON TEMPERATURE

The Compton temperature T_C, that is, the temperature at which heating due to Compton scattering and cooling due to the inverse Compton effect balance, is given by

$$T_C = \frac{h\bar{\nu}}{4k} ,$$

where $h\bar{\nu}$ is the mean photon energy, weighted by the appropriate cross section, and k is Boltzmann's constant (see Levich and Sunyaev 1971; Guilbert 1986). For energies above $\sim$50 keV, relativistic corrections to the scattering yield become important (see Guilbert 1986); for this regime (50 keV $\leq$ 100 MeV), a numerical fit to Winslow's (1975) results, kindly provided by Dr. C. B. Tarter, were used.

In this section we derive the Compton temperature of the radiation field deduced above, and we then consider the effects of changing the high-energy portion of this field.

a) *T_C for the Mean Radiation Field*

We have computed T_C for the "mean" radiation field. The results are summarized in Table 1, which indicates the percentage contribution of each continuum segment to the Compton heating (col. [4]) and cooling (col. [5]) rates. The continuum longward of 1 μm dominates the cooling, and the continuum near 50–200 keV dominates the heating. The resulting temperature is $T_C \approx 9.7 \times 10^6$ K.

We will show below that this low temperature has several consequences, which together eliminate Compton equilibrium as the governing agent for the physical conditions in the BLR. This low value of T_C is the major result of this paper, so we will consider first some alternatives to the continuum we have used.

There are two major differences between our continuum and that used, for instance, by Krolik, McKee, and Tarter (1981) in their seminal paper on the hot phase. The first is our much flatter optical and ultraviolet continuum, which serves to increase the relative infrared flux and hence its effects on the Compton cooling rate. There is now good evidence that a good fraction of the energy budget of a typical AGN is emitted in the infrared (see Elvis *et al.* 1984; Malkan 1984). The second, and major, source of difference, is in our choice of an X-ray to γ-ray continuum similar to the average AGN; Krolik *et al.* used 3C 273 as a template, and it is now known that the high-energy

TABLE 1

CONTINUUM SHAPE

Interval (1)	Energy (eV) (2)	Slope (3)	Heat (%) (4)	Cool (%) (5)
1.........	0.00124–2.8	1.0	0.	46.8
2.........	2.8–23.7	0.5	0.08	23.8
3.........	23.7–56.2	1.0	0.17	15.2
4.........	56.2–365	3	0.25	8.60
5.........	365–10^5	0.7	35.4	4.87
6.........	10^5–10^8	1.67	64.0	0.72

emission from this quasar is anomalously strong. The continuum we have chosen is both similar to that seen in AGNs (Zamorani *et al.* 1981) and consistent with limits to the 100 keV–0.4 MeV flux set by considerations of the X-ray and γ-ray background (Rothschild *et al.* 1983).

b) Two Limits to the Compton Temperature

The temperature of the hot phase is especially sensitive to the radiation field between 50 keV and 500 keV (see Table 1). The shape of this part of the continuum is not well determined; in this section we consider the effects of changing the assumed continuum shape between two extreme limits.

The energy of the "break" in the hard X-ray–soft γ-ray continuum (where the spectral index changes from ~ 0.7 to ~ 1.7) is not well determined. Only three objects (3C 273, Cen A, and NGC 4151) have been detected at these energies; Cen A does not show a break at observed energies (see Gehrels *et al.* 1984) while 3C 273 cannot be representative of AGN if the X-ray background is not to be exceeded. In its high state, NGC 4151 has a break at ~ 50 keV. To test the effects of an especially hard continuum, we have computed T_C for the case where the X-ray continuum extends to 100 MeV with a spectral index of 0.7. This continuum is in clear violation of background limits (Rothschild *et al.* 1983) but does characterize some extreme objects, and serves to indicate an extreme upper limit to T_C. The result is $T_C \approx 4.6 \times 10^7$ K.

A lower limit to T_C is found by considering a softer X-ray continuum; Zamorani *et al.* (1981) find several cases where $\alpha_{ox} \approx 1.6$. If we assume a local X-ray spectral index of 0.7, $\alpha_{ox} = 1.6$ and join the high-energy continuum at 100 keV, the resulting value of T_C is 2.8×10^6 K. Even this temperature is high because it now appears that some AGN are characterized by X-ray continua with significantly softer slopes, sometimes as steep as 2.2 (Elvis *et al.* 1985). A combination of steep α_{ox}, and X-ray continuum, would produce Compton temperatures well below 10^5 K, with the exact result dependent on the treatment of the infrared continuum.

Apparently then, the hot phase of broad-line objects, if it is at the Compton temperature, can have temperatures in the ranges $0.1\text{–}46 \times 10^6$ K, with $T \approx 10^7$ K most likely.

IV. OPTICAL DEPTH CONSEQUENCES OF A LOW T_C

In this section we discuss some implications the Compton temperature deduced above has upon the optical depth of the hot intercloud medium (HIM). Photoionization models (Davidson 1977; Kwan and Krolik 1981) suggest that BLR clouds have $N_H \approx 10^{9.5}$ cm^{-3} and $T_e \approx 2 \times 10^4$ K at their inner edge. If $T_{HIM} \equiv T_C \approx 10^7$ K for typical quasars then the density of the hot phase must be $\sim 6 \times 10^6$ cm^{-3}. Defining an ionization parameter U as the ratio of the photon to hydrogen densities, the ionization parameter deduced for the BLR is $\log U_{BLR} \approx -2$ and the corresponding ionization parameter for the HIM is $\log U_{HIM} \approx 0.7$. The low ionization parameter and high density of the hot phase have observational consequences which effectively rule out the existence of an intercloud medium at the Compton temperature.

a) Calculations

Figure 2 shows the results of a photoionization calculation using the continuum shown in Figure 1. The effects of the radiation between 1 μm and 100 MeV are included on the ionization and heating of gas containing the elements H, He, C, N, O, Ne, Mg, Al, Si, S, Ar, Ca, and Fe with relative proportions 10^5, 10^4, 47.0, 9.8, 83.0, 10.0, 4.20, 0.27, 4.30, 1.70, 0.38, 0.23, and 3.3, respectively. The calculation is straightforward and uses methods and assumptions very similar to those outlined in Krolik, McKee, and Tarter (1981). (Tests show that the present photoionization code gives predictions in excellent agreement with Krolik *et al.* when the same continuum is used.) Parameters were chosen to produce an ionization parameter of $\log U = -2$ for a density of $\log N_H = 9.5$, i.e., the ionizing ($\lambda \geq 912$ Å) photon flux was kept constant at $\phi = 9.486 \times 10^{17}$ cm s^{-1} while the hydrogen density was varied. Figure 2 shows the equilibrium temperature, pressure, and fraction of the K-shell electrons present in Fe (i.e., 1 indicates that both electrons are present in 100% of the ions).

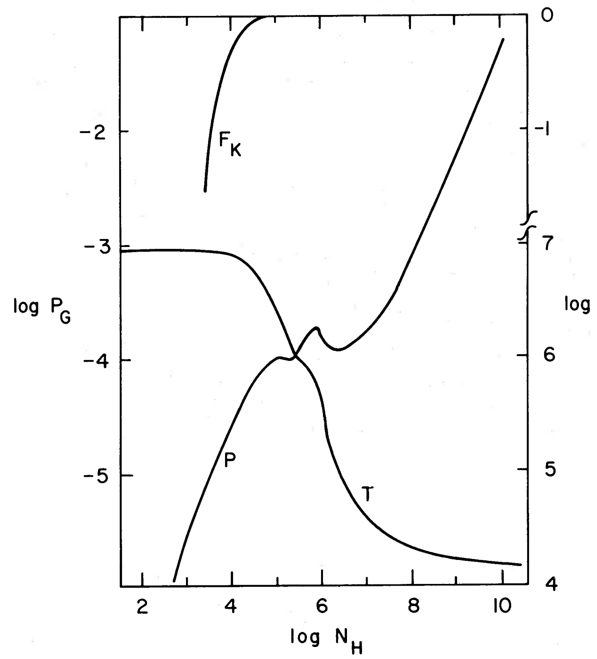

FIG. 2.—Photoionization calculations. Shown are results of a series of calculations in which the hydrogen density was varied and the ionizing photon density was kept constant. Conditions were chosen so that an ionization parameter of $\log U = -2$ was reached at a density of $10^{9.5}$ cm^{-3}. Because of this, the calculations are appropriate for gas at the BLR radius. The electron temperature and gas pressure are shown in lower half of figure. Gas at densities less than 10^4 cm^{-3} equilibriates at the Compton temperature for the radiation field of Fig. 1, $T_C = 9.7 \times 10^6$ K. Upper portion shows fraction of the K-shell of Fe which is filled; unity on this scale indicates that all Fe has at least two electrons. Fe must be fully stripped of electrons if the hot phase is to be optically thin to observed radiations. The Compton temperature is too low by a factor of ~ 100 for this to occur.

b) Consequences of a Low Compton Temperature

The calculation (Fig. 2) does not produce a two-phase equilibrium (that is, the same pressure at two different temperatures) with the correct ionization parameters, a result found, for instance, by Fabian *et al.* (1986). This prediction is very sensitive to details of the atomic data base and elemental composition used, however. This is because the equilibrium conditions for the cool phase are strongly affected by the presence or absence of such cooling ions as Li-like neon. We do not concentrate on these details, which could be altered by other choices of composition, or changes in the atomic data base, but rather draw attention to some global properties of the HIM.

The opacity of an intercloud medium with the parameters given above would be large, with the result that all AGN would be observed to have severe absorption of ionizing radiation. Tests show that Fe K-shell electrons constitute a major opacity source for highly ionized gases when Fe is not fully stripped and Fe is present with a solar abundance. Figure 2 shows that an ionization parameter of at least log $U \approx 3.5$ is needed for Fe to be fully ionized. For typical BLR conditions and $T_C = 10^7$ K, the HIM has log $U = 0.7$ and the K-shell of Fe is fully populated.

It is easy to show that a HIM with $T_C = 10^7$ K would have substantial optical depth to photoelectric absorption. Assuming a solar abundance of two-electron Fe (Fe/H $= 3.3 \times 10^{-5}$), that the density of the hot phase varies as $N_H \propto r^{-2}$ (r is the radius), and a K-shell cross section of 2.3×10^{-20} cm^{-2}, the requirement that the hot phase be optically thin to X-ray radiation sets the limit

$$N_H R_{BLR} < \frac{1}{\sigma \text{ Fe/H}} = 1.3 \times 10^{24} \text{ cm}^{-2}$$

where σ is the photoionization cross section. For a typical quasar BLR radius of $\sim 10^{19}$ cm (see Davidson and Netzer 1979) the corresponding hot-phase density must be $\sim 10^5$ cm^{-3} or less if it is to be transparent to ionizing radiation. This in turn requires that the hot phase have a temperature $\sim 10^{8.7}$ K or higher. Tests show that an intercloud medium with a density of 6×10^6 cm^{-3}, the density needed in the HIM to pressure-support typical BLR clouds if $T_{HIM} \equiv T_C$, would fully absorb all radiation between 13.6 eV and ~ 5 keV. This is a direct consequence of the low Compton temperature and of the resulting low ionization parameter and high density of the intercloud medium. Alternatively, a several order-of-magnitude heavy element depletion could be invoked to alleviate this problem.

V. DYNAMICAL IMPLICATIONS OF A COOL, DENSE INTERCLOUD MEDIUM

The economy in achieving both the clouds and their confining medium by exposure to the same radiation field has been responsible for the wide acceptance of this model of the BLR. Not only were both thermal and mechanical equilibria obtained in this two-phase scheme, it was anticipated that this condition would be reached for densities and pressures in the dense (cloud) phase similar to those required for BLRs in quasars and active galaxies. In addition, the initial theoretical studies of this model did not address important questions concerning the mechanism and time required to establish the two phases involved nor how the desired mass fraction of the two phases would arise in any particular situation. The global dynamical consequences of this model, which we discuss here, have also not received sufficient attention. It is in consideration of the line-broadening dynamics that the model encounters its most severe and invalidating constraints.

In this section, we assume clouds are confined by a medium having a temperature $\hat{T} \ll 10^{10}$ K, consistent with $\hat{T} \approx 10^7$ K derived in previous sections and referred to here as a "cool" confining medium. (In the following, variables having circumflexes [e.g., $\hat{T}$] refer to properties of the intercloud medium; unadorned variables refer to properties of the clouds.) We begin by establishing that the broad-line clouds are Rayleigh-Taylor unstable if they move at nontrivial velocities relative to the cool confining medium. The clouds (or their optically thin remnants following Rayleigh-Taylor breakup) must therefore be essentially frozen into the cool intercloud medium which dominates the mass of the entire region. Finally, the shared motion of the two phases, when constrained to produce the observed emission-line profiles, is inconsistent with the observed emission-line spectrum and introduces a number of new inconveniences and paradoxes. We conclude that the cloud model is most plausible if the confining medium approaches or exceeds relativistic temperatures.

a) Clouds and Cool Intercloud Gas Must Move Together

Unless the clouds and the intercloud medium are both free-falling together, selective radiative and gravitational forces on the clouds must generate a relative motion between the two phases. When the intercloud medium is cool, a very small relative radial velocity $\Delta u = |u - \hat{u}|$ results in Rayleigh-Taylor (R-T) breakup in the effective gravitational field established by drag forces. The deceleration due to the drag force $g_d = \hat{n}(\Delta u)^2/nr_c = T(\Delta u)^2/\hat{T}r_c$, is always directed from the dense cloud into the confining medium of lower density, an unstable arrangement. Here $r_c \approx 10^{12}$ cm is a typical cloud dimension and pressure balance $nT = \hat{n}\hat{T} \approx 10^{13}$ cm^{-3} K is assumed. Clouds can remain stable to nonlinear R-T instability as they flow through the BLR provided the free-fall time across the cloud $t_{ff} \approx (2r_c/g_d)^{1/2}$ exceeds the flow time $t_f \approx R/u$, where R and u represent characteristic global dimensions and velocities of the BLR. For R-T stability,

$$\frac{\Delta u}{u} < \left(\frac{2\hat{T}}{T}\right)^{1/2} \frac{r_{cl}}{R} \approx 4 \times 10^{-5} r_{c12} R_{18}^{-1} \hat{T}_7^{1/2} ,$$

a condition which cannot obtain unless the clouds are essentially comoving with their environment. It is true that R-T instability can be avoided when radiation and dynamical pressures act together on a cloud (Mathews 1986), but even in this favorable case $\Delta u \leq 200 \hat{T}_7^{1/2}(nT)_{13}^{1/2}$ km s^{-1} is required. It is easy to show that the terminal velocity Δu_t for clouds subject to typical radiative forces (and ignoring R-T breakup) is of this same order. The terminal relative velocity is reached when the radiative acceleration (associated with the absorption of UV photons with each recombination) $g_r \approx 1.8 n\alpha h\nu_0/Mc$ equals g_d, i.e., $\Delta u_t = 140(n_9 \hat{T}_7 r_{c12})^{1/2}$ km s^{-1}, so R-T instability is encountered long before Δu_t is reached. Therefore, relative cloud-intercloud velocities Δu must be very much less then typical broad-line velocities to avoid R-T breakup. Unless their motion relative to the intercloud medium is highly subsonic, variations in the boundary pressure on the cloud can lead to distortion and disruption (Nulsen 1986). Following R-T fragmentation, Δu must be even less for the smaller remnant clouds. We conclude that the cool intercloud model requires that the line-emitting clouds be essentially frozen into the confining medium. Although the line emission arises from the cloud component, the frozen-in condition requires that the kinematics of the broad-line profiles are determined by the motion of the intercloud gas.

The likely prospect of R-T instability makes it difficult to maintain coherency and high column depth in optically thick emission lines throughout the clouds' motion across the profile-producing region. As the R-T instability is occurring in an accelerated broad-line cloud, the fragments produced have a range of sizes and are spread out along the trajectory of the cloud since drag forces are more effective on smaller cloud remnants. If the path of the ensemble of cloud fragments were precisely radial, the systemic optical depth would be unaffected. However, any otherwise negligible nonradial perturbation on the radially moving system of remnants is likely to expose the entire system to undiluted continuum radiation, and the characteristic emission spectrum should be dominated by ions from a highly ionized plasma. This loss of optical depth is a serious problem for the cool intercloud medium. Advocates of cloud motion in such a medium may need to devise an alternate means of producing broad lines from ions in optically thick zones, such as Mg II.

Moreover, when $\hat{T} \leq 10^9$ K the total mass of the intercloud medium $\hat{M}$ exceeds that of the cloud system M_c:

$$\frac{\hat{M}}{M_c} \approx \frac{4}{3}\pi R^3 \frac{(nT)^2}{T\hat{T}} \frac{e_{H\beta}}{L_{H\beta}} \approx 130(nT)_{13}^2 R_{18}^3 T_4^{-1} \hat{T}_7^{-1} L_{H\beta 10}^{-1} .$$

Here $e_{H\beta}$ ergs cm^3 s^{-1} is 10 times the case B rate coefficient for producing Hβ emission at typical (quasar) luminosities of $L_{H\beta 10} = L_{H\beta}/10^{10} L_\odot$.

b) *Dynamical Constraints on the Intercloud Medium*

We conclude that the cool intercloud medium must itself move in such a manner to produce the emission-line profiles as it carries the emitting clouds along. Therefore the radiative conditions that permit the desired two-phase medium and the appropriate level of ionization must exist over spatial and velocity ranges that include the entire broad-line profile. In particular, we assume in the following that the confining medium moves radially at high velocity 5000 km s^{-1} or more. The alternative model of generating broad-line profiles by rotational motion about a central mass concentration is vulnerable to a number of criticisms (Shields 1978*a*, *b*; Mathews 1986) and will not be considered here.

For simplicity in demonstrating the dynamical constraints on radial flow, we consider the motion of the intercloud medium near a large point mass M_h; an additional distributed (stellar) mass contribution is not expected to alter the key issues involved. Furthermore, we maintain that large gas velocities can be produced only if the gas temperature $\hat{T}$ is either much less than (inflow) or much greater than (outflow) the virial temperature $\hat{T}_v = GMM_h/6kR$, where M is the proton mass. Should $\hat{T} \approx \hat{T}_v$, the velocity of the intercloud medium $\hat{u}$ and its embedded clouds would be too slow to account for the broad lines.

The equations that describe steady radial flow are

$$\dot{m} = 4\pi R^2 \hat{n} M \hat{u} , \tag{1}$$

$$\hat{u}\frac{d\hat{u}}{dR} = -\frac{GM_h}{R^2} - \frac{1}{\hat{\rho}}\frac{(2\hat{n}k\hat{T})}{dR} , \tag{2}$$

and

$$\frac{d\hat{T}}{dR} = \frac{2}{3}\hat{T}\frac{1}{\hat{n}}\frac{d\hat{n}}{dR} + \frac{F(\hat{T})}{\hat{u}} , \tag{3}$$

where

$$F(\hat{T}) = \frac{4\sigma_T}{3mc^2}\frac{L}{4\pi R^2}(T_C - \hat{T}) - \frac{\hat{n}\Lambda}{3k} . \tag{4}$$

In view of the remaks above, in equation (2) we consider either the gravitational term (when $\hat{T} \ll \hat{T}_v$) or the pressure gradient term (when $\hat{T} \gg \hat{T}_v$), but not both together. The first term on the right-hand side of equation (3) represents the temperature gradient expected due to the compression or expansion of the gas. The final term in equation (3) is an approximation to the Compton heating-cooling and optically thin radiative emission that characterize the equilibrium of the low-density intercloud medium phase. Here $T_C = h\bar{\nu}/4k$ is the Compton temperature, and L is a representative luminosity of the central source. To simplify the discussion further, we consider only emission by bremsstrahlung, $\Lambda = \lambda_B \hat{T}^{1/2}$, where $\lambda_B = 2.4 \times 10^{-27}$ in cgs units. This theoretical model for the intercloud flow is clearly approximate, but it is sufficient for our purposes here in illustrating the pitfalls of ignoring important gas dynamical features of the problem.

If the dynamical terms are ignored, the equilibrium temperature of the gas is found from $F = 0$, i.e.

$$\hat{T}_{eq} = T_C \delta[(1 + \delta^{-1})^{1/2} - 1]^2 , \tag{5}$$

where

$$\delta = \left(\frac{\lambda_B mc^2 \pi}{\sigma_T Lk}\right)^2 \frac{4}{T_C} \hat{n}^2 R^4 . \tag{6}$$

Solutions of equations (1)–(3) must satisfy a number of important conditions if the cool intercloud medium dynamically accounts for the BLR. (i) The pressure of the intercloud medium, $\hat{n}\hat{T}$, must compress clouds to $n \geq 10^9$–10^{11} cm^{-3} over the range in R where the emission line profile and spectrum are generated. (ii) Reasonable emission-line profiles must result. (iii) The value of the "bolometric" ionization parameter,

$$U_B = \frac{L}{4\pi R^2 \hat{n} c(4kT_C)} = 0.48 L_{46} R_{18}^{-2} \hat{n}_7^{-1} T_{C7}^{-1} , \tag{7}$$

must conform approximately to the above value typical of the BLR and should not vary too much across the emission-line profile. (iv) The mass flow rate $\dot{m}$ must not exceed reasonable astronomical expectations. (v) If the two-phase thermal equilibrium model is correct, the compression term in equation (3) should be small and $\hat{T} \approx \hat{T}_{eq}$ should hold over most of the BLR without additional assumptions. (vi) All of the above must hold for parameters characteristic of both quasars and active galaxies.

c) *Inflow Solutions*

Inflow solutions of equations (1)–(3) are determined by a single differential equation in $d\hat{T}/dR$; the density gradient in equation (3) can be expressed in terms of the velocity gradient by differentiating equation (1). The velocity gradient depends principally on the gravitational term since the pressure gradient term in equation (2) can be neglected.

We begin with a description of an intercloud inflow appropriate to quasar parameters. Our initial conditions at large R are chosen so that an inward integration reaches a typical broad-line velocity $u \approx 5000$ km s^{-1} at $R_{18} \approx 1$. A difficulty arises, however, in simultaneously matching the value of the radiation equilibrium temperature $\hat{T}_{eq}$ with the appropriate ionization parameter U_B in the BLR. Equations (5)–(7) indicate that $\hat{T}_{eq}$ and U_B depend on $\hat{n}R^2$ in a counteractive fashion. This is clear from Table 2, in which values of U_B and $\tau_{eq} = \hat{T}_{eq}/T_C$ are listed for expected values of $\eta \equiv \hat{n}_7 R_{18}^2$. If the two-phase thermal equilibrium is maintained in the BLR, we expect $\tau_{eq} \approx 1$ for values of η corresponding to $U_B \approx 1$, as required by equation (7). For quasar parameters, $L_{46} \approx 1$ and $R_{18} \approx 1$, it is clear from columns (2) and (3) of Table 2 that the parameter η is restricted to a very small range of values near $\eta \approx 0.05$; any $\eta \approx 0.1$–1.0 would have been acceptable, but τ_{eq} is less

TABLE 2

INTERCLOUD PARAMETERS IN THE BROAD-LINE REGION[a]

	$L_{46} = 1$[b]		$L_{46} = 0.01$[b]		$L_{46} = 1$[c]		$L_{46} = 0.01$[c]		
η[d] (1)	U_B (2)	τ_{eq}[e] (3)	U_B (4)	τ_{eq}[e] (5)	U_B (6)	τ_{eq}[e] (7)	U_B (8)	τ_{eq}[e] (9)	$\dot{m}$[f] ($M_\odot$ yr^{-1}) (10)
0.0001	(4810)	1.00	(48.1)	0.81	(481.)	1.00	4.8	0.93	0.16
0.0003	(1610)	0.99	(16.)	0.53	(160.)	1.00	1.6	0.82	0.49
0.001	(481.)	0.98	4.8	(0.16)	(48.1)	0.99	0.48	0.52	1.65
0.003	(161.)	0.94	1.6	(0.024)	(16.0)	0.98	0.16	(0.17)	4.95
0.01	(48.1)	0.81	0.48	(0.0022)	4.8	0.94	(0.048)	(0.021)	16.5
0.03	(16.1)	0.53	0.16	(0.00025)	1.6	0.82	(0.016)	(0.0024)	49.5
0.1	4.8	(0.16)	(0.048)	(2.2–5)	0.48	0.52	(0.0048)	(2.2–4)	165.
0.3	1.6	(0.023)	(0.016)	(2.5–6)	0.16	(0.17)	(0.0016)	(2.5–5)	495.
1.0	0.48	(0.0022)	(0.0048)	(2.2–7)	(0.048)	(0.21)	(0.00048)	(2.2–6)	1650.
3.0	0.16	(0.0003)	(0.0016)	(2.4–8)	(0.016)	(0.02)	(0.00016)	(2.5–7)	4950.

[a] Astronomically inappropriate values are enclosed by parentheses.
[b] $\eta \equiv \hat{n}_7 R_{18}^2$.
[b] $T_C = 10^7$ K.
[c] $T_C = 10^8$ K.
[d] $\eta \equiv \hat{n}_7 R_{18}^2$.
[e] $\tau_{eq} = \hat{T}_{eq}/T_c$.
[f] With $\hat{u} = 5000$ km s^{-1}.

than unity over most of this range. (When $T_C = 10^8$ K, a wider range of η is allowed.)

We therefore choose initial values at an initial radius R_0 such that $\eta = 0.059$ at $R = 10^{18}$ cm. With $R_0 = 1.73 \times 10^{21}$ cm = 563 pc, free fall generates $\hat{u} = (2GM_h/R)^{1/2} = 5000$ km s^{-1} at $R = 6.9 \times 10^{17}$ cm in the BLR, with $M_h = 6.5 \times 10^8$ $M_\odot$. The initial velocity at R_0 is assumed to be 100 km s^{-1}, characteristic of the smallest resolved velocities in broad-line profiles. The gas temperature at R_0 is assumed to be in radiative equilibrium $\hat{T}(R_0) = \hat{T}_{eq}$. These values correspond to $\dot{m} = -79$ $M_\odot$ yr^{-1} according to equation (1).

The results of this inflow calculation are shown in Figure 3 and demonstrate that $\hat{T}$ remains less than $\hat{T}_v$ at all R; this is consistent with neglecting the pressure gradient term in the equation of motion. Also $\hat{T} \approx \hat{T}_{eq}$ is an excellent approximation throughout the flow, including the BLR near $R \approx 10^{18}$. At R_0 Compton heating balances bremsstrahlung cooling very efficiently (so that the $F/\hat{u}$ term in eq. [3] dominates the compression term). When an initial thermal equilibrium is not assumed, $\hat{T}$ very rapidly returns to $\hat{T}_{eq}$. Figure 3 also illustrates both the density $\hat{n}$ in the intercloud flow and the density of the embedded clouds $n_{cl} = (\hat{n}\hat{T})/T$, assuming $T = 1 \times 10^4$ K.

Foremost among the difficulties of this model is the sensitivity of the parameters in the BLR to the starting values at large R. In a real quasar, how would the gas at ~ 500 pc "know" what physical values to assume which lead to the observed conditions at $R = 10^{18}$ cm? In addition to this difficulty, the emission-line clouds do not achieve appropriate broad-line densities ($n \geq 10^8$ cm^{-3}) until $R \approx 1.4 \times 10^{18}$ cm, where the inflow velocity is already $u \approx 3500$ km s^{-1}. This would produce a characteristic peculiarity in the broad-line profiles within 3500 km s^{-1}; emission lines which are enhanced at high cloud densities, such as the Balmer lines, would probably exhibit flatter emission-line cores than those observed. The emission line for free-falling plasma having an emissivity proportional to the density is $L_\nu \propto 1/(\nu - \nu_l)$ photons s^{-1} Hz^{-1}, where ν_l is the rest frequency at line center. This is more sharply peaked than most observed profiles.

Also problematical is the "narrow" line radiation that the intercloud gas emits on its inward flow; the expected luminosity in Hβ in the region $R > 6.6 \times 10^{19}$ cm (corresponding to $\hat{T} < 10^5$ and $\hat{u} < 52$ km s^{-1}) is $L_{H\beta} \approx 4 \times 10^8$ $L_\odot$ for conditions shown in Figure 3. Therefore, on this model the intercloud medium should always generate an observable narrow-line component, although narrow lines are absent in many quasar spectra. If the intercloud medium were clumpy at large R, the narrow-line emission from it would be even larger for fixed $\dot{m}$.

Next we consider the intercloud inflow for parameters characteristic of Seyfert galaxies, $L_{46} = 0.01$, and $R \approx 10^{17}$ cm. The expected range in U is similar to that of quasars, but appropriate values of η are ~ 100 times less. Columns (4) and (5) of Table 2 indicate that the ranges of acceptable values of U_B and $\tau_{eq} = \hat{T}_{eq}/T_C$ are again narrowly restricted for $T_C \approx 10^7$ (but less so for $T_C \approx 10^8$). As before, the limited range of broad-line parameters can be reached by a carefully chosen set of initial flow parameters at $R_0 = 1.74 \times 10^{20}$; $\dot{m} = -0.792$ $M_\odot$ yr^{-1}, $\hat{u}_0 = 100$ km s^{-1}, and $M_h = 6.5 \times 10^7$ $M_\odot$ with $L_{46} = 0.01$.

The result of the Seyfert intercloud inflow shown in Figure 4 qualitatively resembles that for quasar parameters, except at small R the gas is significantly heated by compression in excess of the equilibrium value $\hat{T}_{eq}$ due to the radiative terms alone. Deep within the BLR, at $R = 1 \times 10^{16}$ cm for example (where $\hat{u} = 13{,}000$ km s^{-1}) $\hat{T} = 2.4 \times 10^7$ K while $\hat{T}_{eq} = 6.8 \times 10^6$ K. In applying this model to Seyferts, we would generally expect the gas radiating at the wings of the lines to have temperatures determined more by dynamic compression than by the two-phase radiative equilibrium model for which $\hat{T} = \hat{T}_{eq}$ strictly holds. Owing to the greater compression of the embedded clouds, the ionization parameter in Seyfert line wings would also be expected to be systematically lower than those for quasars, but this is not observed. The hydrodynamic term in equation (3) is more important relative to the radiative source terms for Seyferts as compared to quasars. Although the Compton heating time $t_C = 3mc^2\pi R^2\hat{T}/\sigma_T(\hat{T}_C - \hat{T}) \approx 40R_{18}^2 L_{46}^{-1}\hat{T}/(\hat{T}_C - \hat{T})$ yr is similar for Seyferts and quasars, the flow time across the BLR $t_f \approx 3R/2\hat{u} \approx 90R_{18}(\hat{u}/5 \times 10^8)^{-1}$ yr is comparable to t_C for quasars, but it is significantly less than t_C in Seyferts. Besides these special difficulties

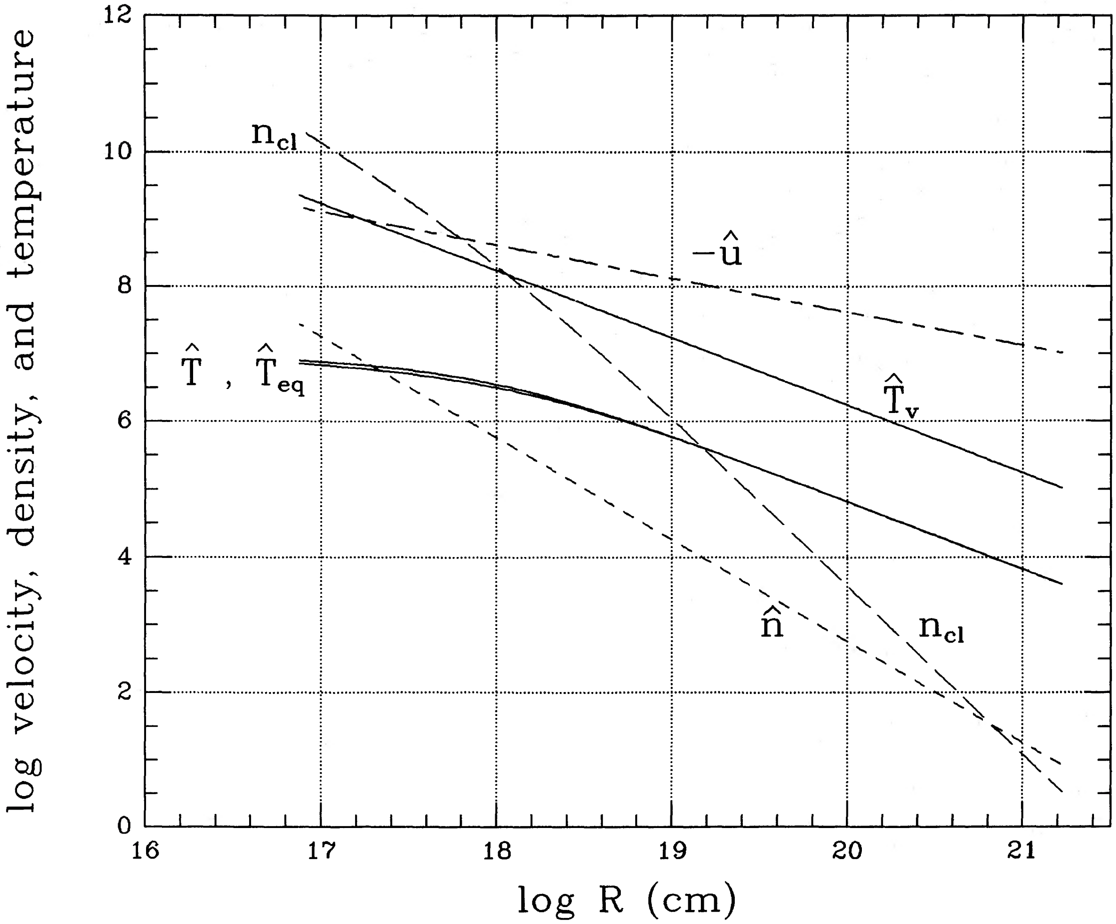

FIG. 3.—Variation of intercloud flow for quasar luminosity $L_{46} = 1$. *Solid lines:* temperature curves; gas temperature $\hat{T}$ lies just above equilibrium temperature $\hat{T}_{eq}$, and $\hat{T}_v$ is the virial temperature. *Short-dashed curve:* density of the intercloud medium; *long dashed curve:* density n_{cl} of embedded broad-line clouds. *Long- and short-dashed curve:* (negative) flow velocity $-\hat{u}$.

for Seyfert parameters, the intercloud inflow model suffers from additional difficulties discussed earlier for the quasar case.

d) Outflow Solutions

We assume that strong outflow occurs when $\hat{T} \gg \hat{T}_v$ for which the gravitational term in equation (2) can be neglected. In this approximation, equations (1)–(2) reduce to two coupled differential equations:

$$\frac{d\hat{T}}{dR} = \frac{1}{\hat{u}} \frac{[F(\hat{u}^2 - \kappa\hat{T}) - (4\hat{T}\hat{u}^3/3R)]}{(\hat{u}^2 - 5\kappa\hat{T}/3)}, \tag{8}$$

and

$$\frac{d\hat{u}}{dR} = \frac{\kappa[(10\hat{T}\hat{u}/3R) - F]}{(\hat{u}^2 - 5\kappa\hat{T}/3)}, \tag{9}$$

where $\kappa \equiv 2k/M$. These equations formally allow a critical or sonic radius R_c (at which both numerators vanish) allowing solutions to pass through the (adiabatic) sonic point. However, sonic solutions can only occur when the kinematic luminosity in the BLR, $\dot{m}\hat{u}^2/2$, is a very small fraction ($\lesssim 10^{-4}$) of the bolometric luminosity L, which is unlikely to be satisfied for most cases of interest. In any case, the high Mach number of the outflow, equal to $12(\hat{u}/5 \times 10^8)\hat{T}_7^{-1/2}$, suggests that the intercloud medium moves supersonically throughout the broad-line region as long as $\hat{T} \approx \hat{T}_{eq}$ and $\hat{T}_{eq} < 10^9$ K, as required by the observed continuum spectra in the Compton two-phase model.

We consider an outflow for quasar parameters evolving according to equations (8) and (9). The flow begins at the base of the BLR $R_0 = 10^{17}$ cm, where $\hat{u} = 5000$ km s^{-1} is assumed. By Table 2, η is again closely restricted to values near 0.05. Unfortunately, the inequality $\hat{T} < \hat{T}_v$ can be satisfied only if $M_h \leq 10^6\ M_\odot$. This unrealistically small central mass—when compared to the enormous luminosities of quasars—reveals an important inconsistency in the marriage of the radiatively heated two-phase medium and the gas dynamical outflow model.

Ideally, a successful intercloud outflow model should begin with a relatively slow-moving wind beneath the BLR which is subsequently accelerated by pressure gradients to broad-line velocities. Unfortunately, this cannot be achieved in practice within the physical and astronomical limitations of equations (8) and (9). Consider, for example, a quasar wind beginning at $R_0 = 10^{17}$ cm with velocity $\hat{u} = 500$ km s^{-1}, density $\hat{n} = 5 \times 10^7$ cm^{-3}, and $\hat{T} = \hat{T}_{eq}$. Such an outflow is shown in Figure 5. Although $\hat{T} \approx \hat{T}_{eq}$ is sustained throughout the BLR $R \leq 10^{18}$ cm, a very low central mass ($M_h = 1 \times 10^6\ M_\odot$) is required to maintain $\hat{T}_v < \hat{T}$. In addition, the gas velocity $\hat{u}$ does not increase to observed values in the BLR, reaching only 840 km s^{-1} at $R \approx 10^{18}$ and rising to a terminal value of

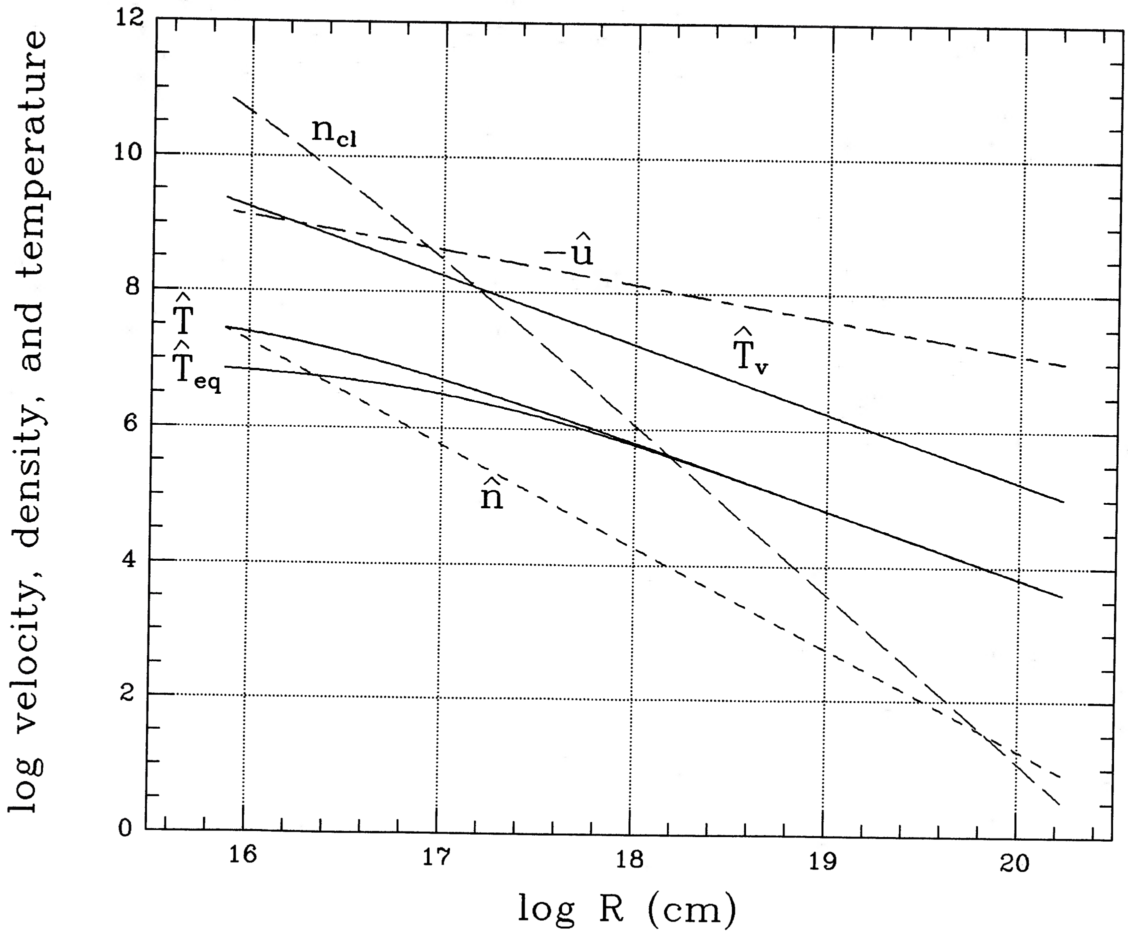

FIG. 4.—Intercloud inflow for Seyfert luminosity $L_{46} = 0.01$. Lines labeled as in Fig. 3

1280 km s^{-1} at larger R. The thermal energy stored in the intercloud gas at $\hat{T} \approx \hat{T}_{eq} \approx 10^7$ K is insufficient to generate broad emission-line profiles extending to 10^4 km s^{-1}.

An attempt to avoid this difficulty by increasing the temperature (by non-Compton processes or perhaps by stimulated Compton heating) at the base of the BLR to values in excess of $\hat{T}_{eq}$ may fail to produce any steady outflow at all. For example, $\hat{T} = 10^9$ drives a steady outflow provided $u = 5000$ km s^{-1} initially (as shown in Fig. 6), but higher $\hat{T}$ (with $\hat{u} = 5000$ km s^{-1}) or lower $\hat{u}$ (with $\hat{T} = 10^9$ K) may fail to generate a steady outflow. These difficulties stem from fundamental and rather perverse limitations of unrestrained steady adiabatic flow from a point source. If $T \propto n^{2/3}$ and $F = 0$ in equations (8) and (9), the radius and velocity of the flow are related by

$$\frac{R}{R_0} = \left(\frac{\hat{u}}{\hat{u}_0}\right)^{-1/2} \left\{1 + \lambda\left[1 - \left(\frac{\hat{u}}{\hat{u}_0}\right)^2\right]\right\}^{-3/4}, \tag{10}$$

where $\lambda = \hat{u}_0^2/5\kappa\hat{T}_0$ and all values with subscript zero refer to initial values for the outflow. An examination of equation (10) reveals that initially accelerated outflow, $du/dR > 0$, is only possible when $\lambda > \frac{1}{3}$, otherwise the solutions exhibit unphysical behavior such as double-valued velocities at small R. This restriction on λ is altered somewhat when $F \neq 0$ but the effect is still strongly present in solutions of equations (8) and (9); unless $\lambda \leq \frac{1}{3}$, or equivalently $(\hat{u}_0/5000 \text{ km s}^{-1})^2 \hat{T}_{07}^{-1} \geq 1$, steady outflow cannot be established.

Evidently, thermally driven outflows of a Compton-heated intercloud medium do not naturally produce astronomically acceptable solutions for the BLR. To permit strong outflow, the central masses must have implausibly low values. This can be partially alleviated if the temperature at the base of the flow is assumed to be larger than $\hat{T}_{eq}$, as illustrated in Figure 6. For this flow, M_h could be increased by one order of magnitude without violating $\hat{T}_v < \hat{T}$. But setting $\hat{T}(R_0) > \hat{T}_{eq}$ presupposes that Compton heating is not the most important process within R_0. An additional difficulty with the outflow of cool, nonrelativistic intercloud gas is the inability of thermal pressure gradients to achieve the magnitude and range of the observed velocities. It is also necessary that the optical line emission from the cooled intercloud medium at large R not lead to excessive broad [O III] emission. These difficulties also extend to parameters appropriate to active galaxies.

e) Further Concerns about Cloud Origins and Acceleration

One of the implications of the radiative two-phase model for the BLR is that phase changes can occur on time scales less than the flow time $t_f \approx R/u$. Although the cloud formation time has not been established with a complete nonequilibrium calculation, it is likely to be comparable to the Compton time t_C, which is rarely less than t_f. In addition, an important disruption may be associated with the phase change process. As soon as the first part of the cloud cools to $T \approx 10^4$ K, it will experience a radiative (or gravitational) force and be pushed

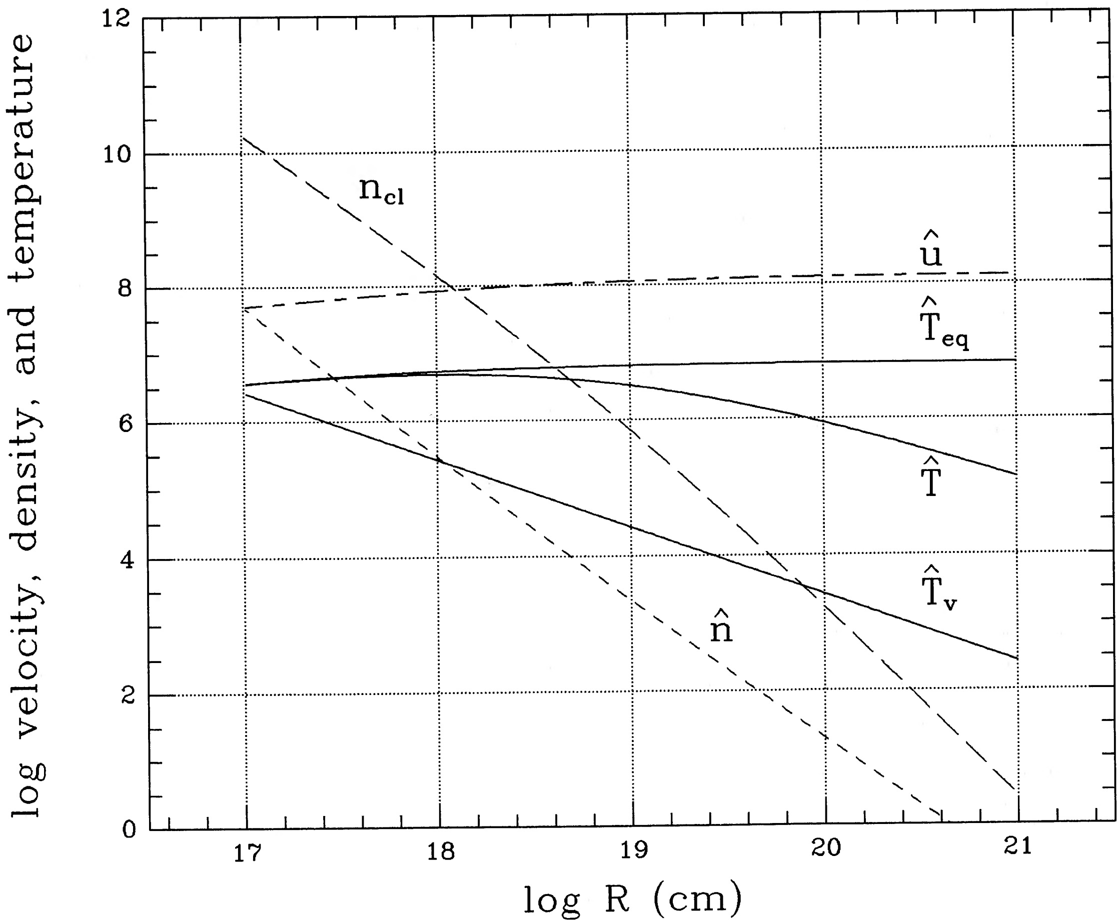

FIG. 5.—Intercloud outflow for quasar parameters and $M_h = 10^6\ M_\odot$ curves are labeled as in Fig. 3

radially away from the center of the cooling perturbation. Subsequent gas that cools is also removed from the densest part of the cooling region in the same manner, so no coherent, approximately spherical cloud can form. The likelihood that this disruptive process occurs is difficult to estimate since it depends on the advanced nonlinear stages of the cooling process, however, it is clear that the phase change process is severely compromised when directional forces (gravity and radiation pressure) are present.

If clouds do not form in any easy manner from condensations in the intercloud medium but instead have some other origin, can they nevertheless be accelerated by the intercloud medium to broad-line velocities? Imagine a cloud which suddenly appears at rest in a radially moving intercloud medium. For simplicity, assume that $\hat{u}$ and $\hat{n}$ are reasonably constant as the cloud is being accelerated. The time required for the cloud to reach velocity $\hat{u}$ is $t_{acc} \approx \hat{u}/g_d \approx (\hat{T}/T)(r_c/\hat{u})$. But this exceeds by $\sim(\hat{T}/T)^{1/2} \approx 30\hat{T}_7$ the time t_{ff} for development of the nonlinear R-T instability. Therefore, since $\hat{T} \gg T$ always obtains, no cloud can be accelerated from rest to broad-line velocities (in a cool intercloud medium) by the action of drag forces without first becoming R-T unstable.

Taken together, the two arguments in this section imply that although the clouds cannot appear from condensations in the intercloud flow, they must first appear in the flow at the local flow velocity! One possible resolution of this paradox is to assume that the cloud-confining medium is relativistically hot.

VI. DISCUSSION

We have shown that the hypothesis that BLR clouds in quasars are supported by a HIM at the Compton temperature of the radiation field is not consistent with observed properties of quasars. The basic problem is that the Compton temperature is far too low: values of $T_C \sim 100$ times larger are needed if the HIM is to be optically thin to ultraviolet and X-ray radiation for roughly solar abundances.

Some aspects of this work were anticipated by Fabian *et al.* (1986), a paper which appeared after this work was started. Their estimate of T_C was the result of the direct observation of a low-energy excess in an *EXOSAT* spectrum of a Seyfert 1 galaxy. Fabian *et al.* note that the HIM might still exist at T_C if the BLR is not exposed to the extreme ultraviolet peak in the radiation field; this cannot be the case since, in this work, we find that the He II BLR spectrum can only be reproduced if clouds absorb an excess of $\sim$4 Ry radiation.

When dynamical constraints are applied to the radiative two-phase model of the intercloud region, neither radial inflow nor outflow satisfy all the conditions for success listed at the end of § V*b*. For $\hat{T}_{eq} \approx 10^7$ K, the emission-line clouds are essentially frozen into the intercloud medium, any relative motion would give rise to R-T instabilities and produce optically thin remnants which are even more closely bound to the ambient flow. (Another origin for gas emitting broad lines from ions of low ionization levels would then be necessary.)

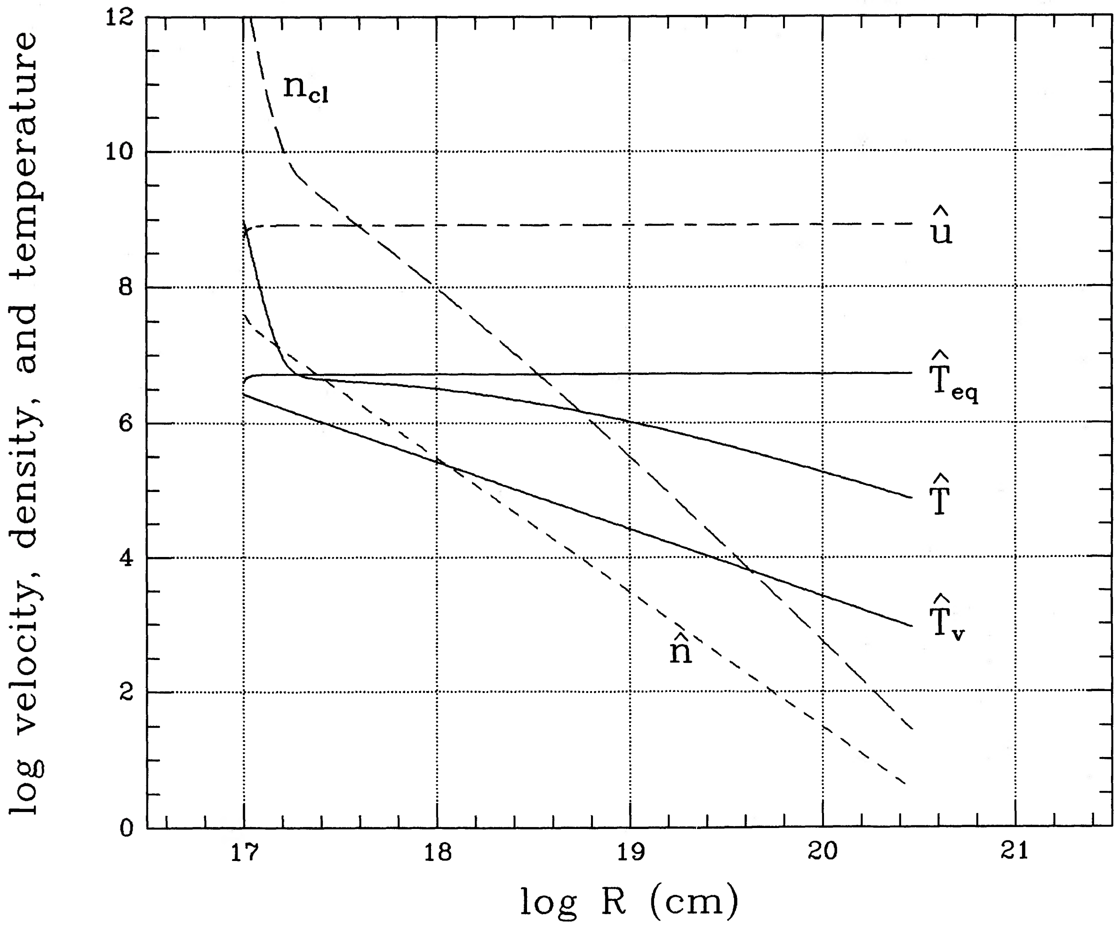

FIG. 6.—Same calculations for intercloud outflow as in Fig. 5 but with $\hat{u}_0 = 5000$ km s^{-1}, $\hat{T}(R_0) = 10^9$ K, and $\dot{m} = 82.6\ M_\odot$ yr^{-1} to maintain $\hat{n}(R_0) = 5 \times 10^7$ as in Fig. 5.

Inflow solutions are very sensitive to initial flow conditions at large radii, give rise to emission-line profiles having peculiar structures and suggest spectral differences between quasars and active galaxies that are evidently not observed. Outflow solutions of the kind considered here require extremely low central masses and are unable to produce emission-line profiles by the action of thermal pressure gradients alone. In general, the idealized conditions which permit a radiatively determined two-phase medium cannot be maintained over a sufficiently large radius to allow the entire emission profile to form. Finally, the radiative two-phase theory does not prescribe the relative fraction of cloud and intercloud gas—this fraction is essential in obtaining the correct emission-line luminosities—nor is it clear how a phase change between the two gases can be accomplished without disruption by differential radiative forces.

In order to incorporate the Compton two-phase model into a self-consistent dynamical model, it will be necessary to include additional sources of energy and momentum which sacrifice the economy of the two-phase approach. The purely spherical geometry of our elementary models provide no accommodation with an accretion disk which might reside at the center, but this is unlikely to interfere with our conclusions unless the entire broad-line region lies very close to the disk.

Many of the difficulties encountered here with a "cool" intercloud medium may be avoided if the clouds are confined instead by a relativistically hot gas. Many quasars and AGBs are observed to have compact radio sources with minimum pressures and spatial extents consistent with the requirements of the broad-line gas (Blumenthal and Mathews 1975). A non-radiating relativistic proton gas may exist in all BLRs. If $\hat{T} \geq 10^9$ K, neither the emission nor the optical depth of the intercloud medium is problematical, and the emission-line clouds are free to move more rapidly relative to the confining medium. In particular, if the clouds are pushed out radially through a relativistic intercloud medium by a combination of dynamical wind force and radiation pressure, they can be accelerated up to broad-line velocities without suffering R-T or lateral flow instabilities (Mathews 1986).

There are many other reasons to doubt that the HIM could be coupled to the radiation field through the Compton effect. There exist a wide diversity of AGN continua, some with quite steep α_{ox} and α_x, and characterized by very low values of T_C (sometimes below 10^5 K). Nonetheless, all have fairly standard BLRs. This suggests that the physical processes controlling the formation and stability of typical BLR clouds is independent of the color of the radiation field. Alternative heating sources (see Mathews 1974) may lead to relativistic intercloud temperatures, or self-gravitating gas, such as in an accretion disk (Shields 1978*b*), might contribute some but not all of the line emission.

We are grateful to Jack Baldwin, Richard Mushotzky, and Martin Gaskell for several informative conversations, and C. B. Tarter for providing the numerical fit to Winslow's Fokker-Planck results. The support of the NSF through grants AST 85-12414 to Ohio State University and AST 83-12971 to UCSC are also acknowledged.

REFERENCES

Arnauld, K. A., *et al.* 1985, *M.N.R.A.S.*, **217**, 105.
Baity, W., Mushotzky, R., Worrall, D., Rothschild, R., Tennant, A., and Primini, F. 1984, *Ap. J.*, **279**, 555.
Baldwin, J. A. 1977, *Ap. J.*, **214**, 679.
Baldwin, J. A., and Netzer, H. 1978, *Ap. J.*, **226**, 1.
Bignami, G. F., *et al.* 1981, *Astr. Ap.*, **93**, 71.
Blumenthal, G. R., and Mathews, W. G. 1975, *Ap. J.*, **198**, 517.
Davidson, K. 1977, *Ap. J.*, **218**, 20.
Davidson, K., and Netzer, H. 1979, *Rev. Mod. Phys.*, **51**, 715.
de Robertis, M., and Osterbrock, D. E. 1986, *Ap. J.*, **301**, 727.
Elvis, M. 1986, *Pub. A.S.P.*, **98**, 148.
Elvis, M., and Lawrence, A. 1985, in *Astrophysics of Active Galaxies and Quasi-Stellar Objects*, ed. J. Miller (Mill Valley: University Science Books), p. 289.
Elvis, M., Willner, S., Fabbiano, G., Carleton, N., Lawrence, A., and Ward, M. 1984, *Ap. J.*, **280**, 574.
Elvis, M., Wilkes, B. J., and Tananbaum, N. 1985, *Ap. J.*, **292**, 357.
Fabian, A. C., Guilbert, P., Arnaud, K., Shafer, R., Tennant, A., and Ward, M. 1986, *M.N.R.A.S.*, **218**, 457.
Gehrels, N., Cline, T., Teegarden, B., Paciesas, W., Tueller, J., Durouchoux, P. and Hameury, J. M. 1984, *Ap. J.*, **278**, 112.
Guilbert, P. W. 1986, *M.N.R.A.S.*, **218**, 171.
Kallman, T. R., and Mushotzky, R. F. 1985, *Ap. J.*, **292**, 49.
Kwan, J., and Krolik, J. 1981, *Ap. J.*, **250**, 478.
Krolik, J., McKee, C. M., and Tarter, C. B. 1981, *Ap. J.*, **249**, 422.
Lepp, S., McCray, R., Shull, J., Woods, D., and Kallman, T. 1985, *Ap. J.*, **288**, 58.
Levich, E. V., and Sunyzev, R. A. 1971, *Soviet Astr.*, **15**, 363.
MacAlpine, G. M. 1981, *Ap. J.*, **251**, 465.
———. 1985, in *Astrophysics of Active Galaxies and Quasi-Stellar Objects*, ed. J. Miller (Mill Valley: University Science Books), p. 259.
MacAlpine, G. M., Davidson, K., Gull, T. R., and Wu, C. C. 1985, *Ap. J.*, **294**, 147.
Malkan, M. A. 1984, in *X-Ray and UV Emission from Active Galactic Nuclei*, ed. W. Brinkman and J. Trumper (Garching bei Munchen: Max-Planck-Institute fur Extraterrestrische Physik), p. 123 (MPE Rept. 184).
Malkan, M. A., and Sargent, W. A. L. 1982, *Ap. J.*, **254**, 22.
Mathews, W. G. 1974, *Ap. J.*, **189**, 23.
———. 1976, *Ap. J.*, **207**, 351.
———. 1986, *Ap. J.*, **305**, 187.
McCray, R. 1979, in *Active Galactic Nuclei*, ed. C. Hazard and S. Milton (Cambridge: Cambridge University Press), p. 227.
Mushotzky, R. F. 1982, *Ap. J.*, **256**, 92.
Mushotzky, R. F., Marshall, F., Boldt, E., Holt, S., and Serlemitsos, P. 1980, *Ap. J.*, **235**, 377.
Netzer, H. 1985, *Ap. J.*, **289**, 451.
Neugebauer, G., *et al.* 1984, *Ap. J.* (*Letters*), **278**, L83.
Neugebauer, G., Oke, J. B., Becklin, E. E., and Matthews, K. 1979, *Ap. J.*, **230**, 79.
Nulsen, P. E. J. 1986, *M.N.R.A.S.*, **221**, 377.
Oke, J. B., Shields, G. A., and Korykansky, D. G. 1984, *Ap. J.*, **277**, 64.
Rothschild, R., Mushotzky, R., Baity, W., Gruber, D., Matteson, J., and Peterson, L. 1983, *Ap. J.*, **269**, 423.
Shields, G. A. 1976, *Ap. J.*, **204**, 330.
———. 1978*a*, in *Pittsburgh Conf. BL Lac Objects*', ed. A. M. Wolfe (Pittsburg: University of Pittsburg Press), p. 257.
———. 1978*b*, *Nature*, **272**, 706.
Smith, M. G., Carswell, R. F., Whelan, J., Wilkes, B., Boksenberg, A., Clowes, R., Savage, A., Cannon, R., and Wall, J. 1981, *M.N.R.A.S.*, **195**, 437.
Spitzer, L. 1978, *Physical Process in the Interstellar Medium* (New York: Wiley).
Uomoto, A. 1984, *Ap. J.*, **284**, 497.
Wills, B., Netzer, H., and Wills, D. 1985, *Ap. J.*, **288**, 94.
Winslow, A. M. 1975, *Lawrence Livermore Lab. Rept.*, UCID-16854.
Zamorani, G., *et al.* 1981, *Ap. J.*, **245**, 357.

GARY J. FERLAND: Astronomy Department, Ohio State University, Columbus, OH 43210

WILLIAM G. MATHEWS: Lick Observatory and Board of Studies in Astronomy and Astrophysics, University of California at Santa Cruz, Santa Cruz, CA 95064